

# UTV: Creating Underwater Video Datasets using Text-to-Video Synthesis with Pixel-wise Annotations

Quang Trung Truong<sup>1</sup> Wong Yuk Kwan<sup>1</sup> Duc Thanh Nguyen<sup>2</sup> Binh-Son Hua<sup>3</sup> Sai-Kit Yeung<sup>1</sup>  
<sup>1</sup>Hong Kong University of Science and Technology  
<sup>2</sup>Deakin University  
<sup>3</sup>Trinity College Dublin

qttruong@connect.ust.hk, ykwongaq@connect.ust.hk, duc.nguyen@deakin.edu.au, binhson.hua@tcd.ie, saikit@ust.hk

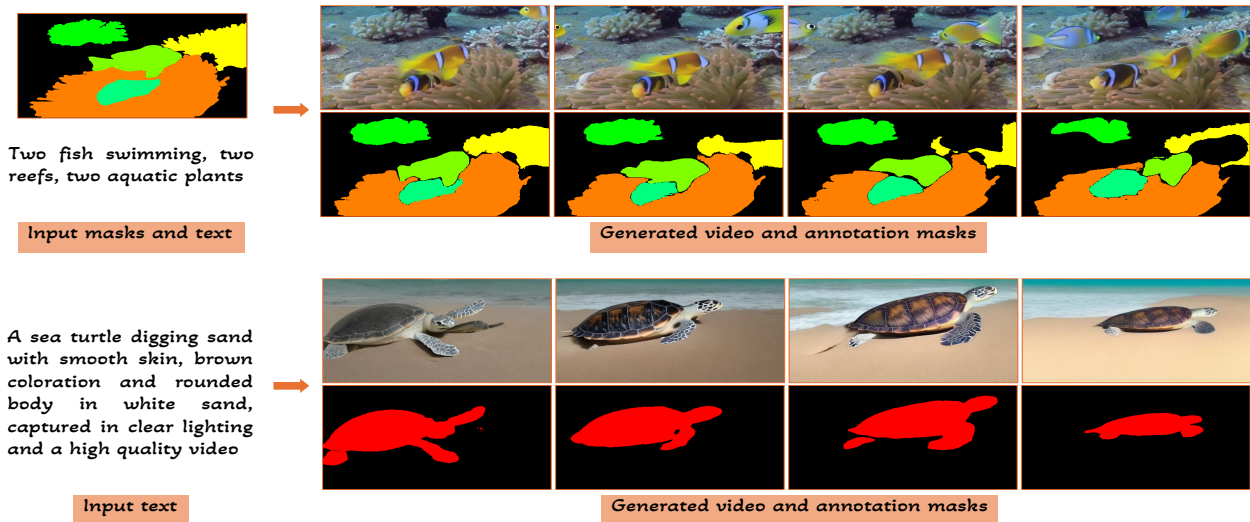


Figure 1. Given masks of the first video frame and a text, or a text, our method synthesizes a high-fidelity video

## Abstract

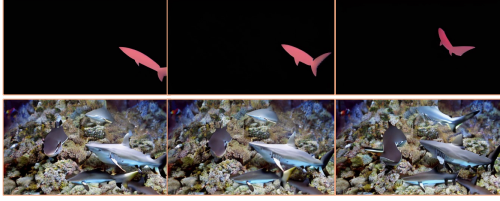
Recent advances in generative AI research for videos, such as SAM2 and text-to-video diffusion models, have demonstrated great potentials to create large-scale datasets with minimal human intervention. In underwater setting, we observe the need for diverse video datasets to capture the unique characteristics of dynamic objects in such an environment that are often absent in generic datasets. In this paper, we propose a new framework for synthesizing videos and pixel-wise annotations tailored for underwater computer vision tasks including video inpainting and video object segmentation. We demonstrate the effectiveness of this framework by constructing two video datasets, namely UTV, a real-world dataset comprising 2,000 video-text pairs, and SUTV, a large-scale synthetic video dataset featuring 10,000 videos and segmentation masks. We show that our synthetic dataset significantly improves the perfor-

mance of downstream methods in video inpainting and self-supervised video object segmentation tasks. Specifically, downstream models are trained on the synthetic dataset and evaluated on real datasets.

## 1. Introduction

Approximately 75% of the Earth’s surface or 362 million  $km^2$  is dominated by oceans and major seas. These vast bodies of water are integral to climate regulation and serve as a primary source of oxygen for the planet. However, marine species are considerably less well-documented compared with land species. Almost 89% of marine protected areas are under-explored [17] and only 200 marine areas are recorded in the World Database on Protected Areas [21].

Underwater video analysis domain focuses on interpreting and understanding of marine video footage, thereby aiding in the exploration and conservation of marine resources.



A big shark chasing a school of fish.

Figure 2. Generated samples by the first T2V solution. Specifically, the T2V model is leveraged to generate annotation masks, which are then used to condition the generation of videos. The generated masks and videos highlight the failure to align the generated segmentation masks with the video.

Literature has shown a large body of research methods devoted to underwater video analysis. For instance, underwater instance segmentation is studied in [10, 11]. FishNet [8] enhances the understanding of ecological marine roles, supporting various vision tasks through experiments conducted on 94,532 images. IOCFomer [28] addresses underwater object counting problem. SAM-based Marine-Inst [43] leverages continuous data annotation by utilizing both human-annotated and model-generated instance masks to improve training data for instance segmentation. Depth estimation and underwater image restoration are studied in [31].

There exist several marine datasets. Specifically, [1] introduces the UTB180 dataset, which contains 180 marine video segments, to benchmark object tracking methods. MVK [29] proposes a marine video dataset that includes 44,330 text-image pairs designed for known item search task. CBIL [36] leverages video-based motion prior to guide the model learn various movement patterns e.g., the counterclockwise circling of sharks. However, CBIL is heavily dependent on the input movement patterns i.e., video segmentation masks to synthesize motions. A Variational Autoencoder (VAE) is used to convert data from pixel spaces into latent spaces, while an adversarial imitation learning approach is employed to accurately capture the intricate movements of schools of fish. In contrast, our approach using image or video mask conditioning, whether included or not, facilitates improved visual fidelity, better motion control and temporal consistency

In this regard, text-to-video synthesis presents a promising approach, providing an innovative way to create informative visual content based on textual descriptions. This technology not only improves the accessibility of marine data but also simplifies species identification and habitat evaluation. We explore two solutions that use T2V models for generating segmentation datasets.

The first one is to adopt a T2V to generate annotation masks, which are then used to condition the generation of videos. For still images, these masks can be efficiently produced by fine-tuning T2I models on COCO instance seg-

mentation [12]. Subsequently, the generated masks serve as input for Mask2Image within the SegGen [41] framework. We establish a baseline by initially generating video segmentation masks, followed by video generation. However, it is not trivial to establish the scheme on videos that fails to ensure the temporal consistency of segmentation masks trained on limited data, and to align masks with video frames in Figure 2. To address this issue, we adopt one of training-free diffusion approaches to evaluate this solution e.g., [25]. Note that plug-and-play methods are often used to enhance the overall quality of off-the-shelf T2V models. Additionally, training-free approach indicates improved appearance fidelity in the marine domain shown in Figure 6. However, employing video temporal smoothing alters video frames, leading to discrepancies with the initial masks and resulting in misalignment between videos and masks. Direct questions arise: (i) *Is it hard to enforce temporal consistency in generated masks while fine-tuning diffusion models on the limited referring VOS datasets?* and (ii) *How to improve mask and video alignment in generated data?* The primary challenge lies in proposing a simple scheme to connect these two types of T2V models for better video-mask alignment.

In the second solution, we observe training a video diffusion model to generate masks on diverse referring VOS datasets, such as Ref-YouTube-VOS [24] (about 6 FPS), Ref-DAVIS17 [9] (about 30 FPS), MeViS [6] (about 30) often fail to reach the temporal consistency in video annotation synthesis. The temporal inconsistency arises from the varying frames per second (FPS) across these datasets. In contrast, off-the-shelf video diffusion models trained on large scale datasets e.g., WebVid-10M [2] leads to generating videos enforcing temporal coherence. To address this challenge, we propose a novel approach that reverses the conventional SegGen [41] workflow. Specifically, we first utilize the video diffusion model to generate the video content, followed by predicting masks using a segmentation model e.g., SAM2 [19] based on the initialized masks of the first frame that is the semi-supervised VOS setting. In our framework, we will specifically focus on *effectively incorporating temporal information into the image-to-video synthesis, ensuring that the first frame and its corresponding mask remain unmodified*. Thus, our method aims not only to improve the temporal alignment of generated masks but contributes to the appearance fidelity.

To summarize, our contributions include:

- We introduce a T2V framework for synthesizing marine videos and annotation masks aiming to automatically generate synthetic data at scale. Our multimodal framework offers flexibility in controlling visual appearance by conditioning on text and the annotation mask of the initial video frame.
- We introduce the large video-text pair dataset for ma-

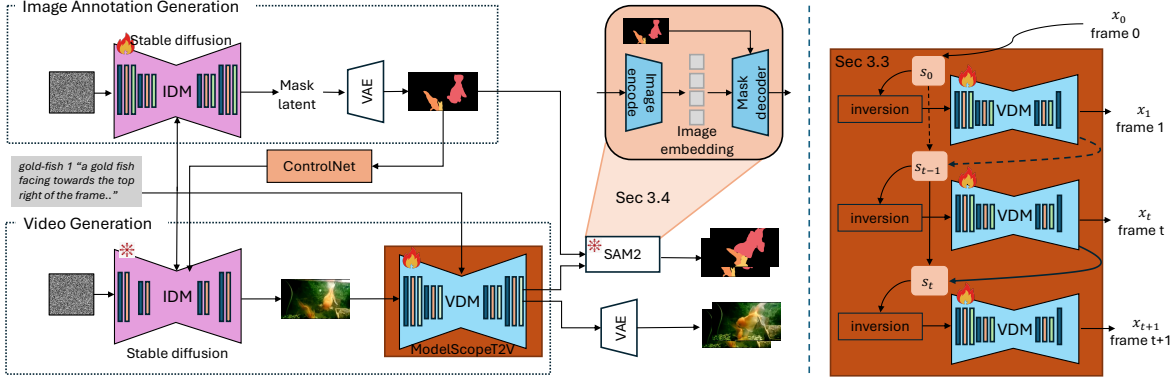


Figure 3. Architecture Overview.

rine applications to facilitate fine-tuning of T2V models. Our findings suggest that training on the UTV dataset enhances video-text alignment of the T2V model [32].

- We present a large-scale synthesis video dataset with pixel-wise annotations. Since marine objects exhibit characteristics similar to dynamic objects and can exhibit camouflage, synthetic dataset shows feature representations leading to improve the performance of leading methods in downstream tasks.

## 2. Related work

**Text-to-Video Generation Models** Diffusion-based text-to-video generation has made significant advancements that is trained on large-scale datasets e.g., WebVid-10M [2], LAION-400M [23]. Make-A-Video [26] employs a two-step approach for text-to-video synthesis that aligns text-to-image and text-to-video tasks by training a single joint foundation model. Notably, images are treated as single-frame videos, enabling the same model to generate both images and videos. Following this line of research direction, Movie Gen [18] builds upon the architecture of image autoencoders proposed by [22], enhancing it by incorporating temporal parameters. This includes a 1D temporal convolution following each 2D spatial convolution and a 1D temporal attention mechanism after each spatial attention layer. The architecture employs temporal downsampling via strided convolution, allowing for the encoding of videos of varying lengths, including images treated as single-frame videos. VideoLDM [3] and ModelScopeT2V [32] extend the 2D-UNet architecture to 3D-UNet by introducing temporal layers and fine-tuning these layers for text-to-video synthesis. [32] is evolved from text-to-image synthesis (T2I) Stable Diffusion (SD) [22] for text-to-video generation.

These two notable open-source T2V models including ModelScopeT2V [32] and VideoCrafter1 [4], have demonstrated significant potential in leveraging their knowledge

to tackle various downstream tasks, thus minimizing or even removing the requirement for extensive labeled data. [33, 34] are developed based on [32]. [14] proposes different attention-based variants, aiming to learn temporal and spatial representations in video inputs.

**Training-free Text-to-Video Generation** Training-free approaches that extend an image foundation model to a video generation model offers an efficient solution, leveraging the generalization capabilities of text-to-image diffusion models trained on larger image data compared to their video counterparts. We observe that this training-free approach in the marine domain often produces high-fidelity videos and achieves better video-text alignment. BIVDiff [25] demonstrates that a training-free approach can excel in several downstream tasks i.e., controllable video generation, video editing, video inpainting, and outpainting. Given the excellent text-image alignment in image foundation diffusion models, BIVDiff [25] utilizes image generation in the first phase, while a video diffusion prior is employed to ensure temporal consistency in the video results. However, the results struggle to effectively control motion information in marine domain.

## 3. Our approach

We introduce UTV, which synthesizes videos and annotations based on text prompt conditioning. Our goal is to fine-tune a text-to-video diffusion model that significantly mitigates text-video alignment issue in marine domain. The generated videos exhibit high visual fidelity, allowing human annotators to vote on rejecting or accepting the synthesized data, thereby enforcing coherence between the text prompts and the resulting video content.

### 3.1. Preliminary: Video Diffusion Model

T2V models e.g., ModelScopeT2V [32], often extend text-to-image diffusion models e.g., Stable Diffusion [22] by in-

tegrating spatio-temporal blocks into the UNet architecture to ensure temporal consistency. T2V diffusion model architecture is divided into three main components: a VAE encoder  $\mathcal{E}$  for translating pixel spaces to latent spaces, a denoising UNet  $\mathcal{U}$  and a VAE decoder  $\mathcal{D}$ . [32] is an open-source model classified as a latent diffusion model and comprises a total of 1.7 billion parameters. Specifically, the denoising UNet model comprises three blocks: the encoder (has 422 million parameters) the middle blocks (has 165 million parameters) including temporal blocks totaling 552 million, and the decoder (756 million parameters).

In general, training T2V model involves two steps including pre-training on text-to-image task, followed by joint training on both text-to-image and text-to-video tasks. The input video is mapped to a latent space via the encoder  $\mathcal{E}$ , which is subsequently perturbed by introducing a small amount of Gaussian noise. Simultaneously, the text prompt is encoded into text embeddings using a pre-trained text encoder. The denoising UNet  $\mathcal{U}$  is optimized to predict the noise and reconstruct the synthesis video data via the decoder  $\mathcal{D}$ , conditioned on the text embeddings.

### 3.2. Latent Image Diffusion Model Generators

We propose a framework that guarantees temporal consistency in the generated masks and improves the alignment between masks and videos. This is accomplished by integrating a strong video diffusion prior into the image-to-video generation process, while preserving the original first frame and its corresponding mask.

**Text-to-Annotation Generation.** Following the fine-tuning phase, we proceeded to generate masks using a text-to-image model e.g., Stable Diffusion-v1.5(SD) [22], which has shown effectiveness in generating high-quality images from textual inputs. The objective was to generate image annotation conditioning that would guide the subsequent video frame generation process. The model [22] was fine-tuned on our marine video frame and text pairs, and benchmark datasets e.g., DAVIS17 [9] Ref-YouTube-VOS 2018 and 2019 [24] to ensure that it could produce masks that accurately represent the content described in the text.

**Conditional Annotation-to-Image Generation.** Conditional image generation aims at synthesizing images based on user-provided signals i.e., annotation masks. Here we generate images that align well with corresponding segmentation masks and text prompts, which serve as the first frames for the synthesis videos discussed in Section 3.3. We use ControlNet [42] feature representations as a guiding signal to employ the SD [22] for image generation conditioned on masks. This dual conditioning allowed for improved coherence in the generated visuals.

### 3.3. Text-to-Video Diffusion Model

Initially, we use a pre-trained text-to-video diffusion model e.g., ModelScopeT2V [32] as our base model that was trained on large-scale datasets demonstrating generalization capability. To adapt the model for marine applications, we fine-tuned [32] using our UTV-2K dataset to ensure effective alignment of text and video on marine domain. We compiled a comprehensive dataset consisting of video clips that showcase marine life, including fish behaviors, coral reef dynamics, and underwater ecosystems.

BIVDiff [25] employs DDIM inversion to adapt an image diffusion model for video diffusion. However, synthesizing the entire video directly using a T2V model often fails to enforce temporal consistency. A solution is to incorporate generative video prior into frame-wise video diffusion results, leading to alterations to the first frame. *In our setting, we keep the first frame and its annotations unchanged.* Thus, we implement a frame-by-frame generation approach during each diffusion model sampling process.

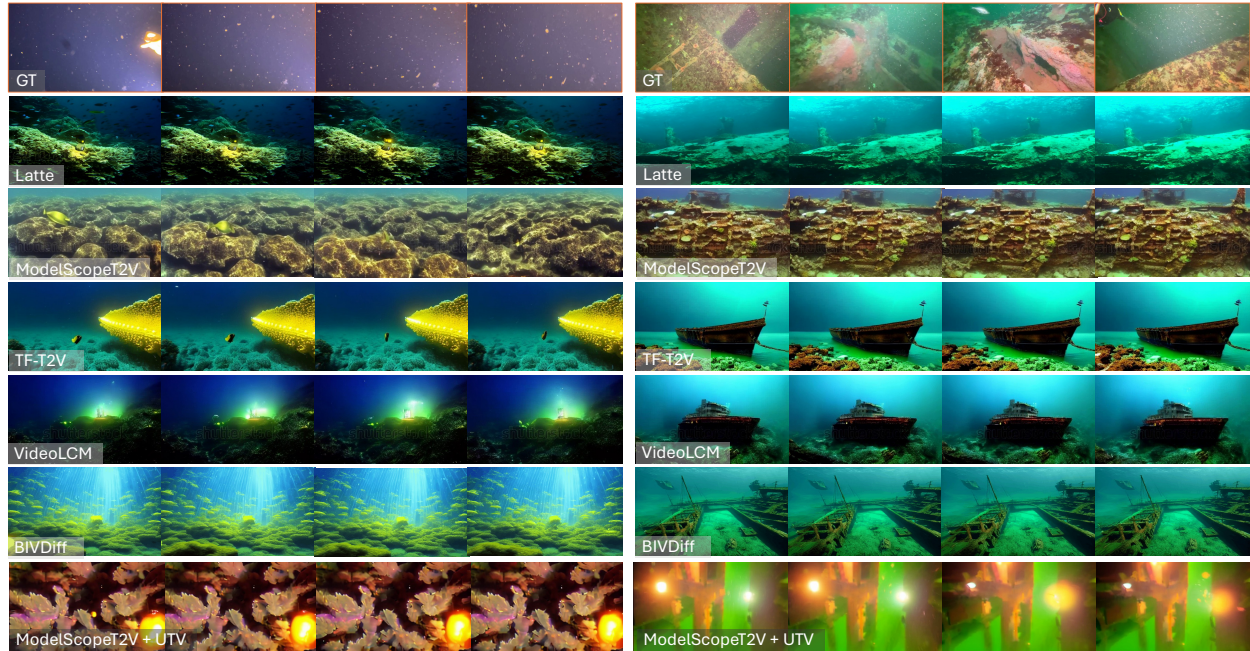
A frame-wise video representation is defined  $s_i[x_0, \dots, x_M]$ , where if  $i = 0$ , then  $x_0$  is synthesized using text-guided, mask-conditioned generation with ControlNet;  $i \in [0, \dots, M - 1]$ . This frame is duplicated for the remaining  $x_i$  to achieve a synthesis video length of  $M + 1$ . We use the encoder  $\mathcal{E}$  to convert frame-wise data  $s_i$  from pixel space to latent space as  $z_0$ .

In the forward diffusion process of the diffusion model, a Markov chain  $z_1, \dots, z_T$  is produced by iteratively adding Gaussian noise to  $z_0$ . The reverse denoising process utilizes a UNet of the fine-tuned ModelScopeT2V to gradually reduce noise in the Markov chain  $z_{T-1}, \dots, z_0$ . We apply DDPM-based inversion to copy frame latent at  $x_M$  to initialize frame latent at  $x_{M+1}$ . We hypothesize that frames  $M$  and  $M + 1$  are closely aligned to reinforce temporal consistency. With generative video prior information, we create videos that ensure this temporal consistency. Finally, the decoder  $\mathcal{D}$  decode the clean latent of the last latent  $x_{M+1}$  as the novel synthesis frame  $x_1$  in Figure 3.

### 3.4. Video Annotation Generator

UTV aims to automatically generate fine-grained video annotations using masks from the first frame. SAM2 [19] requires users to explicitly supply pixel-wise annotations as prompts to guide segmentation. In contrast, the baseline in Figure 7 utilizes bounding boxes from Grounding DINO [20] as prompts for SAM2 in synthesized marine video segmentation. However, the implicit target objects generated by DINO can result in inaccuracies, such as false positives or incomplete segmentation in Figure 7. Consequently, this misalignment hampers the effectiveness of text and mask integration on marine videos. Our image-to-annotation mask diffusion model offers explicit masks of target objects as prompts for SAM2’s prompt encoder. This

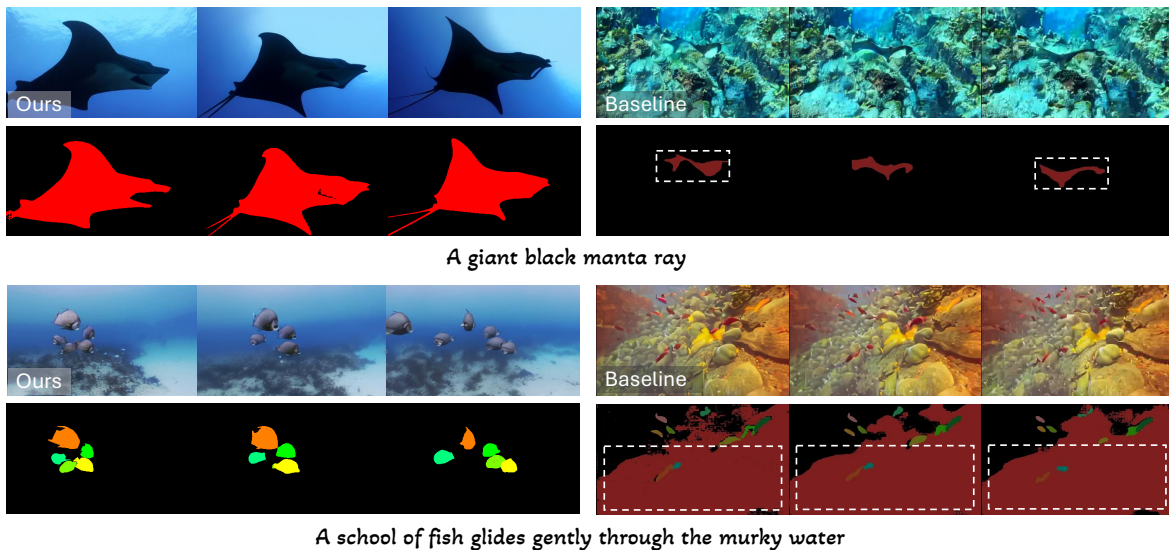




The tiny yellow luminescent creatures reflect light from the diver's torch. Drifting softly in the underwater realm, they create vivid scenery. The panoramic shift from horizontal sweep to tranquil progression engenders a mysterious space

A large, rusty shipwreck lies in the emerald green water at a significant depth, illuminated by flashlights. The high-quality video captures this scene with a panoramic, horizontal view

Figure 6. Qualitative Comparisons.



A giant black manta ray

A school of fish glides gently through the murky water

Figure 7. Qualitative results of our method and a baseline (a T2V model i.e., ModelScopeT2V [32] to generate synthesis videos and Grounded-SAM-2 [20] to predict annotation masks). Text prompts serve as linguistic inputs for predicting annotation masks in the baseline. As shown, the baseline ModelScopeT2V [32] fails to produce high-fidelity video frames, resulting in *partial segmentation* (in the first and second rows). Additionally, DINO's limitations [20] in marine object detection lead to inaccurate box prompts, resulting in *false positives* predicted by SAM2 [19] on marine data (in the third and fourth rows). Our T2V model demonstrates superiority in producing high-fidelity video results and annotations for the first frames (as SAM2 prompts), thereby enhancing the alignment between video and annotation masks.

**Motion filtering** involves removing videos with frequent jittery camera movements, eliminating those that lack mo-

tion, and discarding videos featuring special motion effects in both synthesized videos and annotation masks.

Method	FID↓			FVD↓		
	$\mathcal{S}$	$\mathcal{M}$	$\mathcal{H}$	FVD64↓	FVD128↓	FVD256↓
Latte [14]	110.9	93.7	80.4	4578.1	3699.7	3312.4
ModelScopeT2V [32]	127.4	101.3	92.2	3523.3	3548.5	3426.9
TF-T2V [34]	147.2	136.8	128.2	4843.5	4500.2	4390
VideoLCM [33]	167.5	128.7	126.2	3432.5	3233.6	3018
UTV+ [32]	<b>104.2</b>	<b>87.7</b>	<b>75.7</b>	<b>1506.9</b>	<b>1401</b>	<b>1303.8</b>

Table 2. Quantitative comparison against SOTA methods.  $\mathcal{S}$ ,  $\mathcal{M}$ ,  $\mathcal{H}$  stand for respectively “Simple”, “Medium” and “Hard” as the caption complexity. “Simple”, “Medium” and “Hard” contain 1, 2, more than 2 object attributes, respectively. Best performances are highlighted.

**Visual filtering** focuses on ensuring no watermarks, minimizing scene changes, and maintaining aesthetic quality in the synthesized videos, aiming to produce a high-quality UTV-10K dataset.

To construct the video dataset, we utilize underwater image instance segmentation datasets, such as USIS10K [11] and UIIS [10], along with their respective categories, to condition and text prompts, aiming at generating of synthetic videos and masks. Our multimodal procedure is designed to be flexible, allowing the use of either text prompts or text prompts accompanied by masks as inputs for data synthesis.

USIS10K comprises 10,632 underwater images with pixel-level annotations, while UIIS contains 4,628 underwater images with annotations. We utilize categories as object attributes in our definition within UTV-2K to develop prompt descriptions for generating the synthetic video dataset.

We employ prompts generated from ChatGPT to make the synthesis video, leveraging text prompts as input for the T2V model.

## 5. Experiments

We conducted a comprehensive evaluation of our approach to assess its effectiveness. First, we perform evaluation on T2V models in the marine domain, where we collected both qualitative and quantitative results, uncovering critical insights. We observe that synthetic marine videos generated by T2V models often do not align as effectively with text prompts compared to those produced in more generic domains. Specifically, we leverage the UTV-2K video-text pair dataset for text-to-video synthesis. Next, the UTV-10K synthesis video dataset as augmentation data to improve the performance of downstream task methods.

### 5.1. Implementation Details

We use NVIDIA L20 GPUs for fine-tuning baseline models, testing and generating new data. We fine-tune the T2V model for video synthesis and the T2I model for the baseline in 6 days and 9 days, respectively.

### 5.2. Text-to-Video Synthesis

**Datasets:** To fine-tune ModelScopeT2V [32] for the marine domain, we utilize UTV-2K of 2,000 text-video pairs to enhance the model’s performance. We categorize UTV-2K based on the complexity of their descriptions, defining three levels of difficulty: simple, medium, and hard. Simple videos feature a single central object, medium videos contain two objects within the scene, and hard videos include more than two objects. Our dataset comprises 177 simple videos, 742 medium videos, and 1081 hard videos. To fine-tune SD [22], we use R-VOS datasets including Ref-DAVIS17 [9] with 60 videos, Ref-YouTube-VOS 2018 and 2019 [24] with 2972 videos, and our dataset on the image annotation generation training. We manually annotated 92 underwater videos with pixel-wise labels and accompanying text descriptions to fine-tune the Stable Diffusion model

**Metrics:** To evaluate the performance of our models quantitatively, the Fréchet Video Distance (FVD) [30] and the Fréchet Inception Distance (FID) [7] are used in text-to-video synthesis. We adopted the fixed protocol proposed by StyleGAN-V [27]. The proposed evaluation protocol involves an initial step of sampling the video data and randomly selecting fixed-length video clips from the real data to compute the necessary statistics for assessing the performance of text-to-video generation models.

**Quantitative Analysis:** We initially evaluated T2V models without finetuning on marine data and observed that the synthetic videos did not align well with the text prompts in marine scenarios. We hypothesize that the limited diversity and richness of the marine data utilized for training these T2V models contributes to the observed misalignment. As demonstrated in Table 2, ModelScopeT2V fine-tuned on UTV-2K, significantly outperforms the other models across all metrics.

**Qualitative Analysis:** We qualitatively compare T2V models i.e., Latte, ModelScopeT2V, TF-T2V, and VideoLCM, against free-training models i.e., BIVDiff. Note that we observe the original T2V models often lack the detail and high fidelity found in their free-training counterparts. This discrepancy may be attributed to the integration of powerful T2I models, which generate photorealistic data that aligns more closely with detailed text prompts. For example, Figure 6 illustrates marine objects conditioned on the text prompt “*tiny yellow luminescent creature*”, generated by BIVDiff, are observed in the synthetic video. Furthermore, it is seen that fine-tuning ModelScope on UNDERWATERT2V, preserves details w.r.t text prompts, that closely resembles the ground truth illustrated in Figure 6.

Methods	Real data	Iteration	YouTubeVOS			DAVIS 2016			DAVIS 2017		
			PSNR $\uparrow$	SSIM $\uparrow$	VFID $\downarrow$	PSNR $\uparrow$	SSIM $\uparrow$	VFID $\downarrow$	PSNR $\uparrow$	SSIM $\uparrow$	VFID $\downarrow$
ProPainter [44]	$\checkmark$	700K	<b>33.86</b>	<b>0.9713</b>	<b>0.084</b>	22.90	0.8389	0.946	22.00	0.7965	1.141
[44] + UTV	$\times$	60K	31.82	0.9613	0.117	<b>23.26</b>	<b>0.8493</b>	<b>1.029</b>	<b>22.24</b>	<b>0.7983</b>	<b>1.111</b>

Table 3. Quantitative comparisons on video inpainting. We train ProPainter [44] on respective real and synthetic data, and then evaluate on the real data. We observe training on synthetic data needs fewer iterations than training on the real data. [44] trained on the synthetic data outperforms the original one trained on the real data on DAVIS2016/2017 benchmark datasets. Best performances are highlighted.

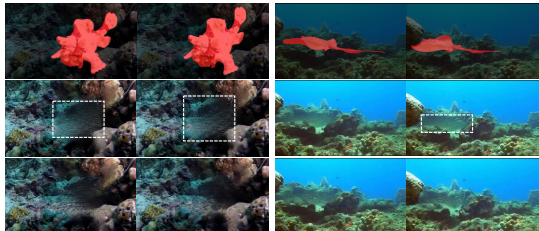


Figure 8. Qualitative comparisons on underwater video inpainting task. We visualize the inpainting results for the original ProPainter [44] (2nd row) and [44] trained on the synthetic data from UTV-2K (3rd row). The masked frames are shown in the 1st row. [44] trained on the synthetic data demonstrates superior performance, producing high-fidelity textures and exhibiting fewer artifacts in the video inpainting results.

**Baseline:** We compare our method with a baseline: a T2V model i.e., ModelScopeT2V [32] and [20]. The T2V model is fine-tuned on the UTV-2K. [20] integrates Grounding DINO [13] and SAM2 for text-guided video segmentation in which Grounding DINO is utilized for marine object detection. We noticed that partial segmentation and false positives appear on DINO [13] leading to fails to detect marine objects on the baseline in Figure 7. While the synthetic data produced by [32] demonstrates good temporal consistency, it struggles to deliver high-fidelity visuals in certain scenarios. Note that we utilize [32] as a generative prior for image-by-image video synthesis.

### 5.3. Application: Downstream tasks

**Video inpainting:** We evaluate propainting methods i.e., ProPainter [44] in Figure 8. We compare [44] trained on a synthetic dataset with the original model trained on benchmark datasets i.e., DAVIS and YTVOS. For a fair comparison, we extract the same length of synthetic video from each video in the DAVIS and YTVOS test sets for evaluation. Our method demonstrates improved performance on the video inpainting task for DAVIS 2016 and 2017 compared to the original ProPainter [44] in Table 3. Additionally, we observe that training on the synthetic dataset leads to significantly faster convergence rates than training from scratch on the real dataset.

**Self-supervised video object segmentation:** Here, we compare methods on self-supervised learning methods using pseudo labels and synthetic data. A straightforward

knowledge distillation (KD) is used to distill AOT and DeAOT variants from the teacher model to the student model, without using ground-truth. Instead of using pseudo labels, AOT and DeAOT are trained on synthetic datasets. We observe that the models trained on the synthetic data outperform KD-based representation learning methods, achieving performance increase of 0.14 to 7.35  $\mathcal{J}\&\mathcal{F}$  on the benchmarking datasets in Table 4.

Method	YouTubeVOS2018	YouTubeVOS2019
	$\mathcal{J}\&\mathcal{F} \uparrow$	$\mathcal{J}\&\mathcal{F} \uparrow$
AOT [40]	67.30	67.60
DeAOT [39]	73.20	74.00
AOT [40]	<b>74.93 (+7.63)</b>	<b>74.95 (+7.35)</b>
DeAOT [39]	74.15 (+0.95)	74.14 (+0.14)

Table 4. Quantitative comparisons on self-supervised video object segmentation. We employ a simple KD scheme to distill feature representations and logits from the largest model to the smallest model in gray color. Models trained on the synthetic data are highlighted in red color. We observe that the methods trained on the synthetic data outperform the KD-based models.

## 6. Conclusion

In this paper, we present a UTV dataset aimed at advancing oceanic research by curating a large-scale collection of real videos paired with high-quality captions. Additionally, we generate 10K synthetic videos with pixel-wise annotations and text descriptions. Our goal is to enhance the understanding of underwater ecosystems by improving data accessibility. We propose an efficient framework for synthesizing videos and annotations that minimizes labeling effort. Our evaluation shows that synthetic data can significantly boost the performance of various downstream tasks. By bridging the gap between synthetic and real data, we aim to foster innovation in computer vision applications e.g., using synthetic data to improve the training phase.

## Acknowledgements

We would like to thank Long Mai for valuable discussions and suggestions; Ziqiang Zheng, Ka Chun Shum, and Yiwei Cheng for their support in technical activities; and Nguyen Minh Hoang, Le Vu Thanh Dat, Nguyen Ngoc Duc, Vo Phu Phong, and Thanh Nghia for their assistance with video annotation and data filtering.



## References

- [1] Basit Alawode, Yuhang Guo, Mehnaz Ummar, Naoufel Werghi, Jorge Dias, Ajmal Mian, and Sajid Javed. Utb180: A high-quality benchmark for underwater tracking. In *Proceedings of the Asian Conference on Computer Vision*, pages 3326–3342, 2022. 2
- [2] Max Bain, Arsha Nagrani, Gül Varol, and Andrew Zisserman. Frozen in time: A joint video and image encoder for end-to-end retrieval. In *Proceedings of the IEEE/CVF International Conference on Computer Vision*, pages 1728–1738, 2021. 2, 3, 5
- [3] Andreas Blattmann, Robin Rombach, Huan Ling, Tim Dockhorn, Seung Wook Kim, Sanja Fidler, and Karsten Kreis. Align your latents: High-resolution video synthesis with latent diffusion models. In *Proceedings of the IEEE/CVF Conference on Computer Vision and Pattern Recognition*, pages 22563–22575, 2023. 3
- [4] Haoxin Chen, Menghan Xia, Yingqing He, Yong Zhang, Xiaodong Cun, Shaoshu Yang, Jinbo Xing, Yaofang Liu, Qifeng Chen, Xintao Wang, et al. Videocrafter1: Open diffusion models for high-quality video generation. *arXiv preprint arXiv:2310.19512*, 2023. 3
- [5] Dima Damen, Hazel Doughty, Giovanni Maria Farinella, Antonino Furnari, Evangelos Kazakos, Jian Ma, Davide Moltisanti, Jonathan Munro, Toby Perrett, Will Price, et al. Rescaling egocentric vision: Collection, pipeline and challenges for epic-kitchens-100. *International Journal of Computer Vision*, pages 1–23, 2022. 5
- [6] Henghui Ding, Chang Liu, Shuting He, Xudong Jiang, and Chen Change Loy. Mevis: A large-scale benchmark for video segmentation with motion expressions. In *Proceedings of the IEEE/CVF International Conference on Computer Vision*, pages 2694–2703, 2023. 2
- [7] Martin Heusel, Hubert Ramsauer, Thomas Unterthiner, Bernhard Nessler, and Sepp Hochreiter. Gans trained by a two time-scale update rule converge to a local nash equilibrium. *Advances in neural information processing systems*, 30, 2017. 7
- [8] Faizan Farooq Khan, Xiang Li, Andrew J Temple, and Mohamed Elhoseiny. Fishnet: A large-scale dataset and benchmark for fish recognition, detection, and functional trait prediction. In *Proceedings of the IEEE/CVF International Conference on Computer Vision*, pages 20496–20506, 2023. 2
- [9] Anna Khoreva, Anna Rohrbach, and Bernt Schiele. Video object segmentation with language referring expressions. In *Computer Vision–ACCV 2018: 14th Asian Conference on Computer Vision, Perth, Australia, December 2–6, 2018, Revised Selected Papers, Part IV 14*, pages 123–141. Springer, 2019. 2, 4, 7
- [10] Shijie Lian, Hua Li, Runmin Cong, Suqi Li, Wei Zhang, and Sam Kwong. Watermask: Instance segmentation for underwater imagery. In *Proceedings of the IEEE/CVF International Conference on Computer Vision*, pages 1305–1315, 2023. 2, 7, 13, 15, 17
- [11] Shijie Lian, Ziyi Zhang, Hua Li, Wenjie Li, Laurence Tianruo Yang, Sam Kwong, and Runmin Cong. Diving into underwater: Segment anything model guided underwater salient instance segmentation and a large-scale dataset. *arXiv preprint arXiv:2406.06039*, 2024. 2, 7
- [12] Tsung-Yi Lin, Michael Maire, Serge Belongie, James Hays, Pietro Perona, Deva Ramanan, Piotr Dollár, and C Lawrence Zitnick. Microsoft coco: Common objects in context. In *Computer Vision–ECCV 2014: 13th European Conference, Zurich, Switzerland, September 6–12, 2014, Proceedings, Part V 13*, pages 740–755. Springer, 2014. 2
- [13] Shilong Liu, Zhaoyang Zeng, Tianhe Ren, Feng Li, Hao Zhang, Jie Yang, Qing Jiang, Chunyuan Li, Jianwei Yang, Hang Su, et al. Grounding dino: Marrying dino with grounded pre-training for open-set object detection. *arXiv preprint arXiv:2303.05499*, 2023. 8
- [14] Xin Ma, Yaohui Wang, Gengyun Jia, Xinyuan Chen, Ziwei Liu, Yuan-Fang Li, Cunjian Chen, and Yu Qiao. Latte: Latent diffusion transformer for video generation. *arXiv preprint arXiv:2401.03048*, 2024. 3, 7
- [15] Ron Mokady, Amir Hertz, and Amit H Bermano. Clipcap: Clip prefix for image captioning. *arXiv preprint arXiv:2111.09734*, 2021. 12
- [16] Haomiao Ni, Bernhard Egger, Suhas Lohit, Anoop Cherian, Ye Wang, Toshiaki Koike-Akino, Sharon X Huang, and Tim K Marks. Ti2v-zero: Zero-shot image conditioning for text-to-video diffusion models. In *Proceedings of the IEEE/CVF Conference on Computer Vision and Pattern Recognition*, pages 9015–9025, 2024. 12
- [17] Elizabeth P Pike, Jessica MC MacCarthy, Sarah O Hameed, Nikki Harasta, Kirsten Grorud-Colvert, Jenna Sullivan-Stack, Joachim Claudet, Barbara Horta e Costa, Emanuel J Gonçalves, Angelo Villagomez, et al. Ocean protection quality is lagging behind quantity: Applying a scientific framework to assess real marine protected area progress against the 30 by 30 target. *Conservation Letters*, page e13020, 2024. 1
- [18] Adam Polyak, Amit Zohar, Andrew Brown, Andros Tjandra, Animesh Sinha, Ann Lee, Apoorv Vyas, Bowen Shi, Chih-Yao Ma, Ching-Yao Chuang, et al. Movie gen: A cast of media foundation models. *arXiv preprint arXiv:2410.13720*, 2024. 3
- [19] Nikhila Ravi, Valentin Gabeur, Yuan-Ting Hu, Ronghang Hu, Chaitanya Ryali, Tengyu Ma, Haitham Khedr, Roman Rädle, Chloe Rolland, Laura Gustafson, Eric Mintun, Junting Pan, Kalyan Vasudev Alwala, Nicolas Carion, Chao-Yuan Wu, Ross Girshick, Piotr Dollár, and Christoph Feichtenhofer. Sam 2: Segment anything in images and videos. *arXiv preprint arXiv:2408.00714*, 2024. 2, 4, 6
- [20] Tianhe Ren, Qing Jiang, Shilong Liu, Zhaoyang Zeng, Wenlong Liu, Han Gao, Hongjie Huang, Zhengyu Ma, Xiaohe Jiang, Yihao Chen, et al. Grounding dino 1.5: Advance the “edge” of open-set object detection. *arXiv preprint arXiv:2405.10300*, 2024. 4, 6, 8
- [21] Julia Roessger, Joachim Claudet, and Barbara Horta e Costa. Turning the tide on protection illusions: The underprotected mpas of the ‘ospar regional sea convention’. *Marine Policy*, 142:105109, 2022. 1
- [22] Robin Rombach, Andreas Blattmann, Dominik Lorenz, Patrick Esser, and Björn Ommer. High-resolution image synthesis with latent diffusion models. In *Proceedings of*

- the *IEEE/CVF conference on computer vision and pattern recognition*, pages 10684–10695, 2022. 3, 4, 7, 11
- [23] Christoph Schuhmann, Richard Vencu, Romain Beaumont, Robert Kaczmarczyk, Clayton Mullis, Aarush Katta, Theo Coombes, Jenia Jitsev, and Aran Komatsuzaki. Laion-400m: Open dataset of clip-filtered 400 million image-text pairs. *arXiv preprint arXiv:2111.02114*, 2021. 3
- [24] Seonguk Seo, Joon-Young Lee, and Bohyung Han. Urvos: Unified referring video object segmentation network with a large-scale benchmark. In *Computer Vision—ECCV 2020: 16th European Conference, Glasgow, UK, August 23–28, 2020, Proceedings, Part XV 16*, pages 208–223. Springer, 2020. 2, 4, 7
- [25] Fengyuan Shi, Jiaxi Gu, Hang Xu, Songcen Xu, Wei Zhang, and Limin Wang. Bivdiff: A training-free framework for general-purpose video synthesis via bridging image and video diffusion models. In *Proceedings of the IEEE/CVF Conference on Computer Vision and Pattern Recognition*, pages 7393–7402, 2024. 2, 3, 4
- [26] Uriel Singer, Adam Polyak, Thomas Hayes, Xi Yin, Jie An, Songyang Zhang, Qiyuan Hu, Harry Yang, Oron Ashual, Oran Gafni, et al. Make-a-video: Text-to-video generation without text-video data. *arXiv preprint arXiv:2209.14792*, 2022. 3
- [27] Ivan Skorokhodov, Sergey Tulyakov, and Mohamed Elhoseiny. Stylegan-v: A continuous video generator with the price, image quality and perks of stylegan2. In *Proceedings of the IEEE/CVF Conference on Computer Vision and Pattern Recognition*, pages 3626–3636, 2022. 7
- [28] Guolei Sun, Zhaochong An, Yun Liu, Ce Liu, Christos Sakaridis, Deng-Ping Fan, and Luc Van Gool. Indiscernible object counting in underwater scenes. In *Proceedings of the IEEE/CVF Conference on Computer Vision and Pattern Recognition*, pages 13791–13801, 2023. 2
- [29] Quang-Trung Truong, Tuan-Anh Vu, Tan-Sang Ha, Jakub Lokoč, Yue-Him Wong, Ajay Joneja, and Sai-Kit Yeung. Marine video kit: a new marine video dataset for content-based analysis and retrieval. In *International Conference on Multimedia Modeling*, pages 539–550. Springer, 2023. 2, 5, 12
- [30] Thomas Unterthiner, Sjoerd Van Steenkiste, Karol Kurach, Raphael Marinier, Marcin Michalski, and Sylvain Gelly. Towards accurate generative models of video: A new metric & challenges. *arXiv preprint arXiv:1812.01717*, 2018. 7
- [31] Nisha Varghese, Ashish Kumar, and AN Rajagopalan. Self-supervised monocular underwater depth recovery, image restoration, and a real-sea video dataset. In *Proceedings of the IEEE/CVF International Conference on Computer Vision*, pages 12248–12258, 2023. 2
- [32] Jiuniu Wang, Hangjie Yuan, Dayou Chen, Yingya Zhang, Xiang Wang, and Shiwei Zhang. Modelscope text-to-video technical report. *arXiv preprint arXiv:2308.06571*, 2023. 3, 4, 6, 7, 8, 11
- [33] Xiang Wang, Shiwei Zhang, Han Zhang, Yu Liu, Yingya Zhang, Changxin Gao, and Nong Sang. Videolcm: Video latent consistency model. *arXiv preprint arXiv:2312.09109*, 2023. 3, 7
- [34] Xiang Wang, Shiwei Zhang, Hangjie Yuan, Zhiwu Qing, Biao Gong, Yingya Zhang, Yujun Shen, Changxin Gao, and Nong Sang. A recipe for scaling up text-to-video generation with text-free videos. In *CVPR*, 2024. 3, 7
- [35] Yi Wang, Yinan He, Yizhuo Li, Kunchang Li, Jiashuo Yu, Xin Ma, Xinhao Li, Guo Chen, Xinyuan Chen, Yaohui Wang, et al. Internvid: A large-scale video-text dataset for multimodal understanding and generation. In *The Twelfth International Conference on Learning Representations*, 2023. 5
- [36] Yifan Wu, Zhiyang Dou, Yuko Ishiwaka, Shun Ogawa, Yuke Lou, Wenping Wang, Lingjie Liu, and Taku Komura. Cbil: Collective behavior imitation learning for fish from real videos. *SIGGRAPH Asia*, 2024. 2
- [37] Jun Xu, Tao Mei, Ting Yao, and Yong Rui. Msr-vtt: A large video description dataset for bridging video and language. In *Proceedings of the IEEE conference on computer vision and pattern recognition*, pages 5288–5296, 2016. 5
- [38] Ning Xu, Linjie Yang, Yuchen Fan, Dingcheng Yue, Yuchen Liang, Jianchao Yang, and Thomas Huang. Youtube-vos: A large-scale video object segmentation benchmark. *arXiv preprint arXiv:1809.03327*, 2018. 11
- [39] Zongxin Yang and Yi Yang. Decoupling features in hierarchical propagation for video object segmentation. In *Neural Information Processing Systems*, 2022. 8
- [40] Zongxin Yang, Yunchao Wei, and Yi Yang. Associating objects with transformers for video object segmentation. In *Neural Information Processing Systems*, pages 2491–2502, 2021. 8
- [41] Hanrong Ye, Jason Kuen, Qing Liu, Zhe Lin, Brian Price, and Dan Xu. Seggen: Supercharging segmentation models with text2mask and mask2img synthesis. *arXiv preprint arXiv:2311.03355*, 2023. 2, 11
- [42] Lvmin Zhang, Anyi Rao, and Maneesh Agrawala. Adding conditional control to text-to-image diffusion models. In *Proceedings of the IEEE/CVF International Conference on Computer Vision*, pages 3836–3847, 2023. 4
- [43] Ziqiang Zheng, Yiwe Chen, Huimin Zeng, Tuan-Anh Vu, Binh-Son Hua, and Sai-Kit Yeung. Marineinst: A foundation model for marine image analysis with instance visual description. In *European Conference on Computer Vision*. Springer, 2024. 2
- [44] Shangchen Zhou, Chongyi Li, Kelvin CK Chan, and Chen Change Loy. Propainter: Improving propagation and transformer for video inpainting. In *Proceedings of the IEEE/CVF International Conference on Computer Vision*, pages 10477–10486, 2023. 8

# UTV: Creating Underwater Video Datasets using Text-to-Video Synthesis with Pixel-wise Annotations

## Supplementary Material

### Abstract

In this supplementary material, we provide detailed descriptions of implementation used in our work in Sec. A. Visualizations of the Variational Autoencoder in generative diffusion models for annotation generation are illustrated in Sec. B. More visual analysis of the first solution is illustrated in Sec. C. Video inpainting ablation is presented in Sec. D. We present an analysis of the real-world video-text dataset in Sec. E. Additionally, we showcase more synthetic datasets generated by our framework in Sec. F. Limitations are discussed in Sec. G.

### A. Implementation details

We fine-tune diffusion models for video generation and annotation mask generation with 25,000 and 30,000 iterations, respectively, using a single NVIDIA L20 GPU. The models are optimized using the AdamW optimizer with a learning rate of  $3 \times 10^{-5}$  and a batch size of 2 for video generation task. The models are conducted at a resolution of  $448 \times 256$ . UTV contain 25 frames in each synthetic video.

### B. Visualizations of Variational Autoencoder (VAE) for pixel-wise annotation reconstruction

We employ VAE in ModelScopeT2V [32] and Stable Diffusion [22] for the encoding and reconstruction of video and image data. We observe VAE effectively encodes and reconstructs annotation maps in Figure 10. Note, videos with very short durations often lead to VAE reconstruction outputs inserting blank frames at the end of the video. While YouTubeVOS videos [38] are recorded at 30 fps, they are annotated at 6 fps, presenting a challenge for VAE reconstruction. To address this problem, we increase the frame rate during video extraction using FFmpeg in fine-tuning diffusion models.

### C. More visual analysis of the first solution

To align video content with annotation maps, we draw inspiration from SegGen [41] for video generation. Specifically, we present the first solution in the main paper which consists of two stages. First, we create a video annotation map. In the second stage, we condition the video generation process on the annotation maps. However, we observe that the generated results with pixel-wise annotations often exhibit artifacts, necessitating improvements to achieve high-quality video outputs

#### C.1. Implementation details

In our first solution, we employ a T2V model i.e., ModelScopeT2V, to generate annotation maps. We utilize an NVIDIA

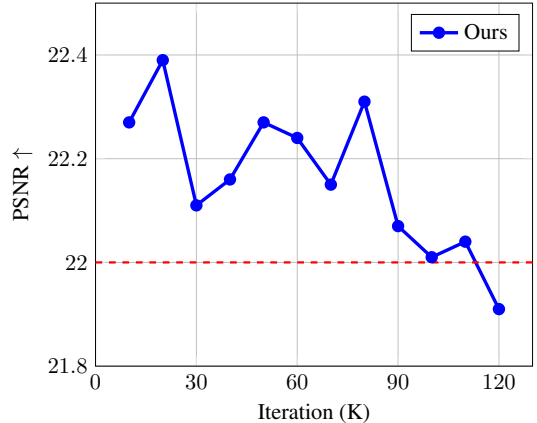


Figure 9. Convergence of video inpainting method on DAVIS2017. We evaluate the performance of ProPainter, trained on synthetic at different training iterations and ProPainter trained on VOS real datasets at iteration of 700K (dash line in red). We observe ProPainter trained on our marine synthetic dataset, achieves faster convergence compared to the model trained on the real datasets. Note, we utilize 25 frames of video sequences for evaluation.

H800 for fine-tuning on the referring VOS datasets and our marine dataset, using an optimizer with a learning rate of  $3 \times 10^{-5}$ , batch size of 8 and a cosine learning schedule over 33,000 iterations.

#### C.2. Visual analysis

This approach leverages T2V to produce annotation maps, which then condition the video generation process. However, we find that ModelScopeT2V generates annotation maps leading to artifacts, including visual jitter, flickering behavior, and instance detection issues in Figure 11. These problems highlight that this solution is not trivial for generating videos with pixel-wise annotations. We suspect that the limited data available for fine-tuning the T2V model is inadequate for demonstrating its generalization capability in data generation.

### D. Video inpainting ablation

We highlight the critical importance of the synthetic dataset for training video inpainting models. We observe that the video inpainting model trained on the synthetic dataset, without access to ground truth labels, outperforms the counterpart trained on the real dataset in Figure 9. Furthermore, training on the synthetic dataset enables the model to achieve faster divergence at earlier iterations (50 iterations vs 700K iterations in ProPainter trained on the real VOS datasets from scratch). This finding is attributed to the unique characteristics of dynamic objects found in our dataset, which are

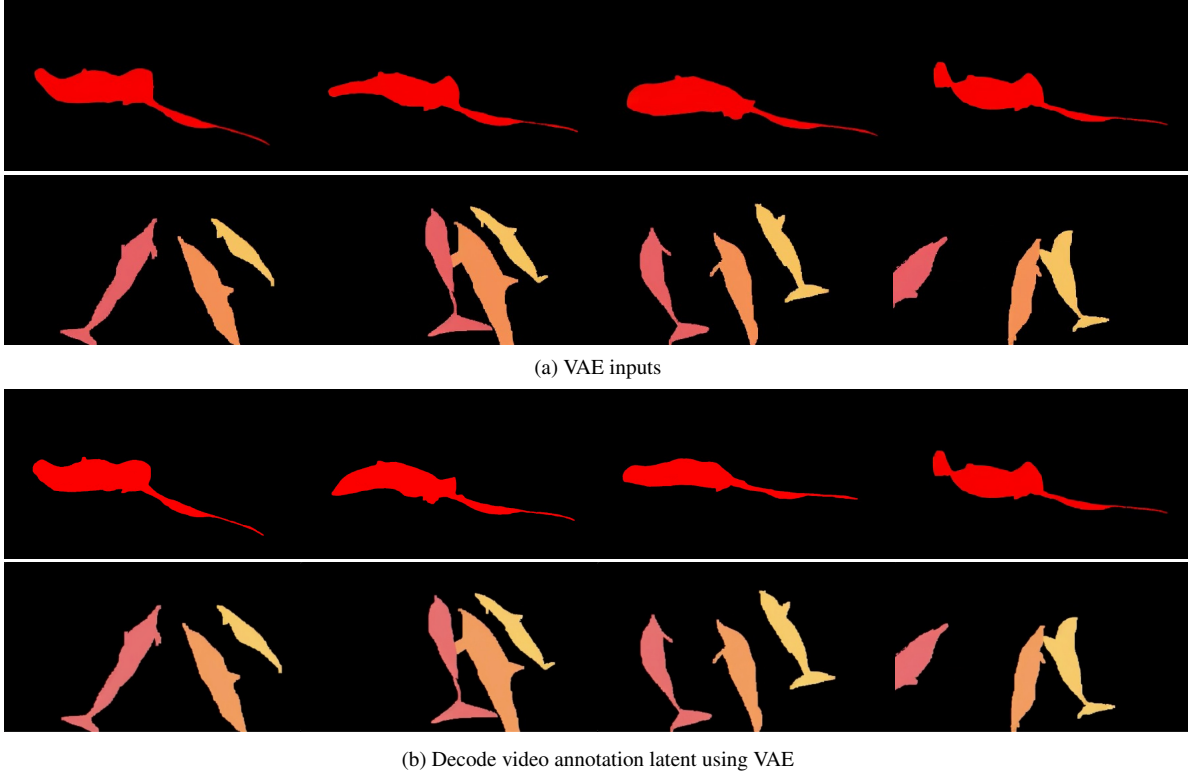


Figure 10. Visual analysis of annotation map reconstruction using VAE. It is noticeable that the VAE shows its effectiveness in encoding and reconstructing video annotation maps. This visualization demonstrates the VAE results in the first solution of the main paper, which adopts a T2V approach to generate video annotation masks.

frequently absent in generic datasets. Downstream models can learn discriminative feature representations, leading to a faster divergence rate.

## E. UTV-2K real video-text dataset

### E.1. Collecting Marine Videos

**Our internal video data.** We have recorded video footage from 8 unique beach/island locations across the four major oceans including Pacific Ocean, Indian Ocean, Atlantic Ocean, Mediterranean Sea, over a 2-year period. Our team has captured a total of hundreds of hours of underwater video footage, but we have specifically selected 18.48 hours of this footage to construct the dataset. Video recordings will focus on a specific area and the activity of marine organisms, with a median duration of approximately 28 seconds. The shortest recording time is 0.46 seconds, while the longest recording is 3.8 minutes. We utilized a variety of camera equipment such as GoPro cameras, and consumer cell-phone cameras.

**MVK dataset.** We have further adopted a public dataset, the MVK [29]. MVK is a marine video dataset comprising 44330 text-image pairs extracted at 1 FPS (frame per second), where the text is automatically generated using [15]. This data was recorded across 11 regions and countries, utilizing a variety of different camera

equipment. The total recording time exceeds 12 hours across 14 unique beach/island locations, with varying recording duration. The median video duration is 29.9 seconds, ranging from 2 seconds to 4.95 minutes.

### E.2. Dataset Split

We categorize our videos based on the complexity of their descriptions, defining three levels of difficulty: simple, medium, and hard. Simple videos feature a single central object, medium videos contain two objects within the scene, and hard videos include more than two objects. Table 5 shows caption examples categorized based on the number of object attributes. We split the dataset into a training set with 1400 videos and a testing set with 600 videos. For the subset, we randomly selected 100 simple videos, 200 medium videos, and 300 hard videos from the dataset.

## F. Additional UTV-10K samples

Recent advances in off-the-shelf generative models have significantly improved data generation. Ni et al. [16] propose an image-to-video synthesis framework conditioned on text prompts to produce temporally coherent videos. Inspired by this work, we adopt ModelScopeT2V model to predict new video frames using generative priors. In our paper, we observe that the solution of generating video annotation masks first and then generating the video is not trivial. To ensure video-annotation alignment, we employ a

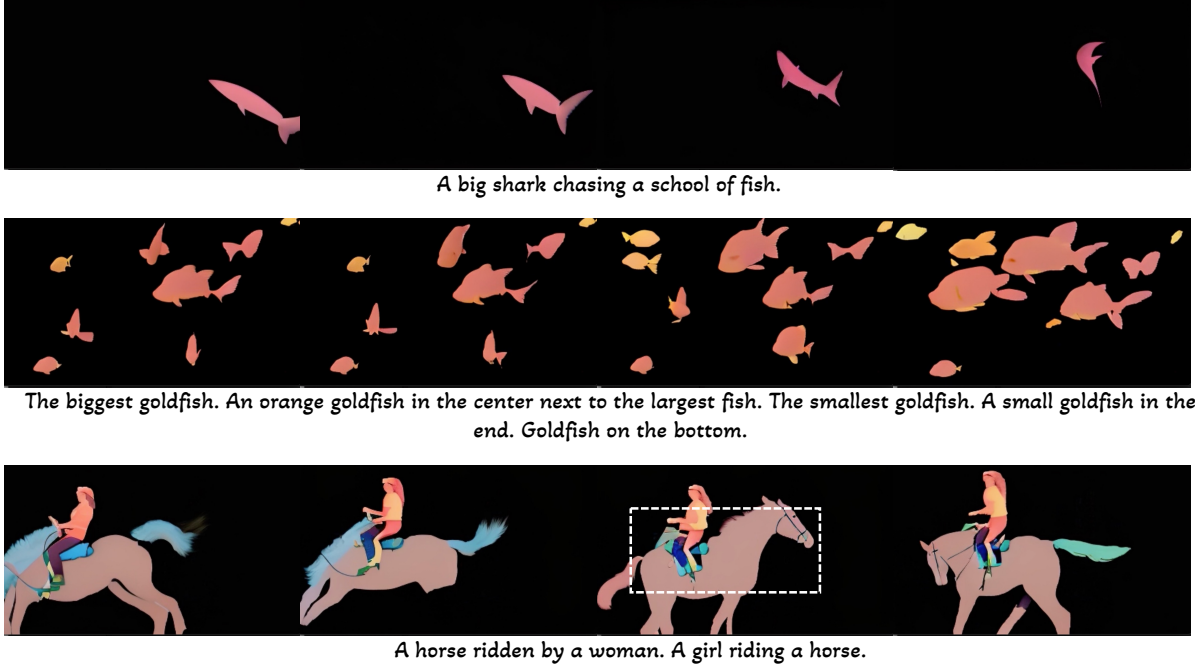


Figure 11. Visualization of the first solution in main paper, that using text-to-video diffusion model aiming at generating annotation maps. ModelScopeT2V generates poor annotation maps, highlighting artifacts in the generated results such as visual jitter (first row), instance object detection issues (second row), and flickering behavior (third row).

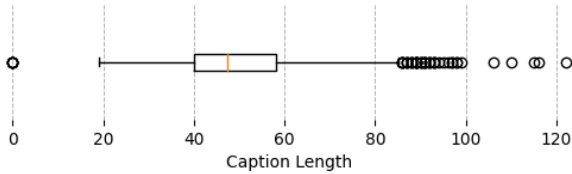


Figure 12. Illustration of caption length over UTV-2K text-video pairs.

diffusion model to generate the video first, followed by effective prediction of the annotation mask.

**Text-to-video synthesis.** Figure 13 illustrates that UTV produces temporally coherent results for different prompts. The video and text are well-aligned in the marine domain.

**Text-to-video synthesis with pixel-wise annotations.** We train and evaluate the diffusion models i.e., ModelScopeTV and SD for pixel-wise annotation map generation using the prompt template: *Generate segmentation maps. < video.description >*.

UTV generates results with natural motion, scenes containing camera changes and object deformation while preserving alignment between the video and annotation masks in Figure 14. Furthermore, we enhance mask-to-video synthesis by leveraging [10] in Figure 15. Our synthetic data showcases a diverse and extensive

array of high-quality training samples.

## G. Discussion and Limitations

UTV has the following limitations that we discuss in this section.

**Scene changes:** We find that our framework generates videos with abrupt scene changes, which is a common artifact in prior generative models. Specifically, generated videos contain several clips, and abrupt scene changes occur at the video shot boundaries. In scenarios where rapid object movements or hallucinated trajectories occur, we often see tracking failures.

**Camera changes:** Another limitation manifests when motion is not initialized in the image-to-video generation. Target objects only appear in the initial frames, resulting in incomplete tracking. We suspect that this issue arises from the absence of temporal guidance in the image-to-video generation process.

**Flickering:** While our framework effectively aligns annotations with the video content, we find it has issues with flickering and visual jitter in Figure 14. Addressing this would be our future work.

Category	Caption
<b>Simple</b>	A large, rusty shipwreck lies in the emerald green water at a significant depth, illuminated by flashlights. The high-quality video captures this scene with a panoramic, horizontal view.
	The sleek, elongated fish swims slowly in the clear brightturquoise water. High quality, captured in sharp detail, with a panoramic shot providing a comprehensive view.
	In the clear brightturquoise water, a school of small Acanthurus blochii fish is swimming in the sea space. The video is recorded in high quality, from panoramic side shots of the entire scene to clear close-ups of the school of fish.
<b>Medium</b>	The rock crevice is gray and rough, with large dimensions and fish swimming around. The water is clear brightturquoise, with medium depth and some light. The video quality is good and clear, with fish swimming slowly. The wide-angle camera pans horizontally around the rock crevice.
	A high-quality video captures a large coral reef with various colors and sizes. Different species of fish, displaying a multitude of colors, swim around in the clear brightturquoise water. The footage provides clear scenes of the surrounding coral reef, with a horizontal angle offering a panoramic view.
	A small striped sea fish with pale brightturquoise color swims around a rocky area. The clear water requires flashlight assistance as sunlight cannot penetrate. The video has sharp clarity, capturing the fish moving slowly from a wide, horizontal panoramic view, highlighting the natural beauty of the marine environment
<b>Hard</b>	Under the ocean floor, the world of branching corals emerges with a mesmerizing jade green hue, where large coral formations densely populate the seabed. Various colorful and uniquely shaped small fish swim around the coral reef. Professional divers control the camera, capturing the scene with the presence of air bubbles. The video records the vivid and lifelike underwater landscape from a high-angle perspective, resembling a painting of the ocean.
	The video captures a large coral reef in brown and mossy colors, surrounded by rocks and marine creatures. Nearby divers and fish swimming around create a lively scene. The clear brightturquoise water, medium depth, and daylight provide a sharp image. The video records the movement of the coral with a wide, horizontal shot
	A clear, high-definition video captures a close-up of a small Bansa fish with a white body and two black stripes, gracefully swimming. Four divers move slowly near an abandoned underwater structure in the clear brightturquoise sea, with a school of small fish swimming around it. The camera pans horizontally around the Bansa fish, capturing the divers and a corner of the structure.

Table 5. Prompts are categorized based on the object attributes given in a textual input. Specifically, there are three prompt examples w.r.t three videos each category. “Simple”, “Medium” and “Hard” contain 1, 2, more than 2 object attributes, respectively. Object attributes are highlighted in red, aiming at categorizing caption prompts.



The mud crabs. They have a hard, brown shell with ridges on the surface. In terms of visual characteristics, their shells are very clean and transparent underwater, allowing the camera to record good quality images. Their movement speed is not fast, allowing the camera to focus on capturing their fine details. With a progressive rotation angle, the camera can easily see clearly every ridge on the crab's body, creating a beautiful and vivid image.



Deep beneath the blue sea, large gray sharks stretch, with small fish trailing behind and coral reefs as the backdrop. The high-quality video captures the slow and free movement of the sharks in front of the camera, while the camera records their entire movement from panoramic to static angles.



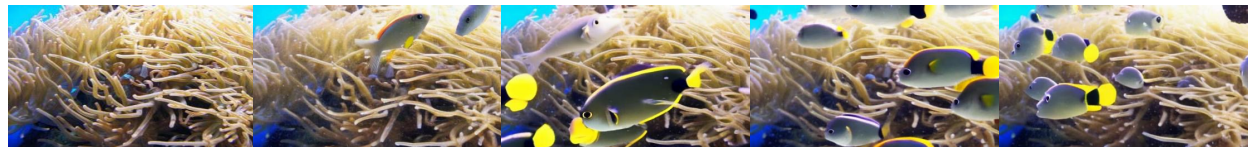
Deep beneath the ocean floor, a large sea turtle with black and gray shell stands still on the coral reef. The high-quality video captures the peaceful image of the turtle, with close-up shots focusing on the turtle's shell, along with static shots.



A fish



Coral reefs



An aquatic plant

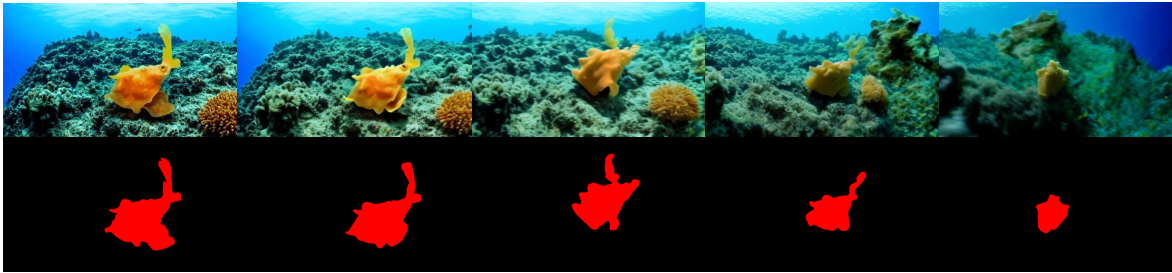


A fish

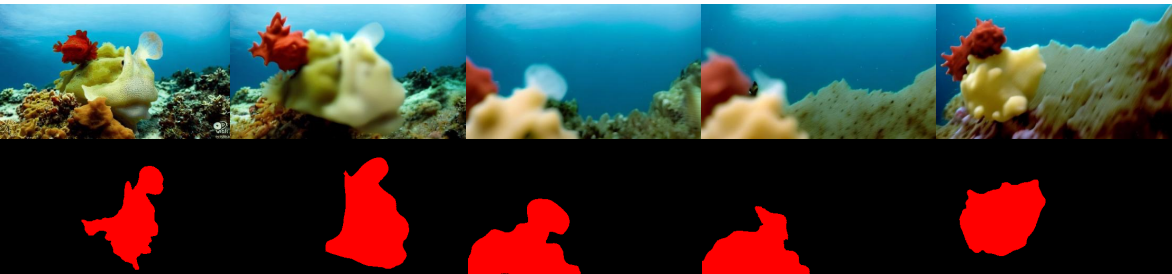


Human divers

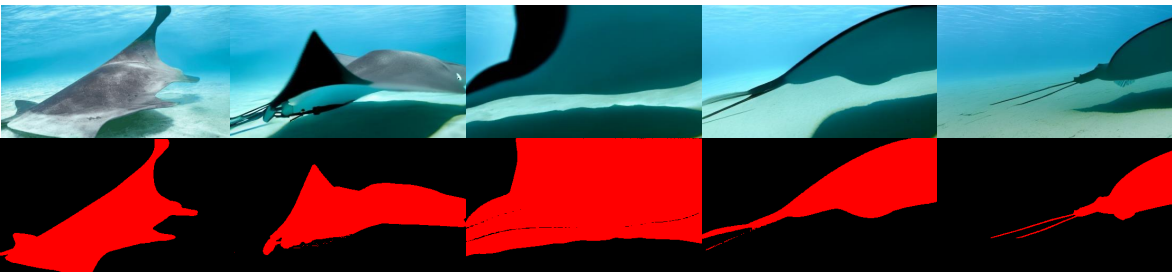
Figure 13. Underwater videos generated from UTV based on the prompts from the UTV test set provided by human annotators (1st to 3rd rows) and categories in UIIS [10] (4th to 8th rows).



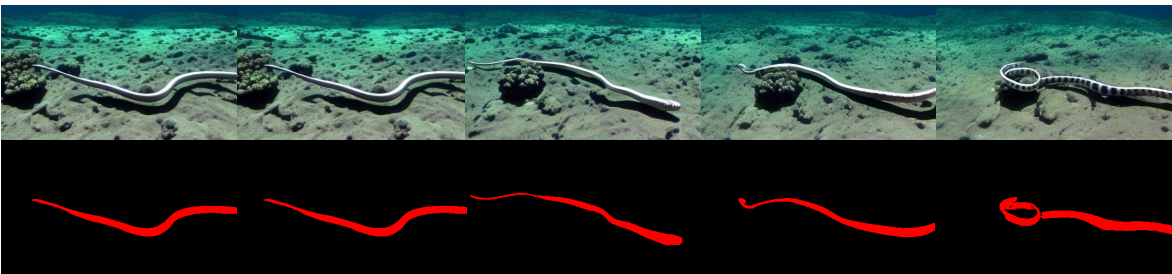
A frogfish with a spongy skin, small size, and reddish coloration beside coral reef underneath the blue water, captured in clear lighting and high-quality video.



A frogfish with a spongy skin, small size, and reddish coloration in a rocky surface with coral reef lies on the seabed, captured in clear lighting and medium quality video.



A swimming stingray with flexible fins, white and disc-shaped in blue water, captured in clear lighting and a high quality video.



A sea snake with smooth skin, black and white banded pattern, was separated with a coral reef system, captured in clear lighting and a high quality video

Figure 14. Samples generated from UTV with the collection of prompts provided by human annotators.



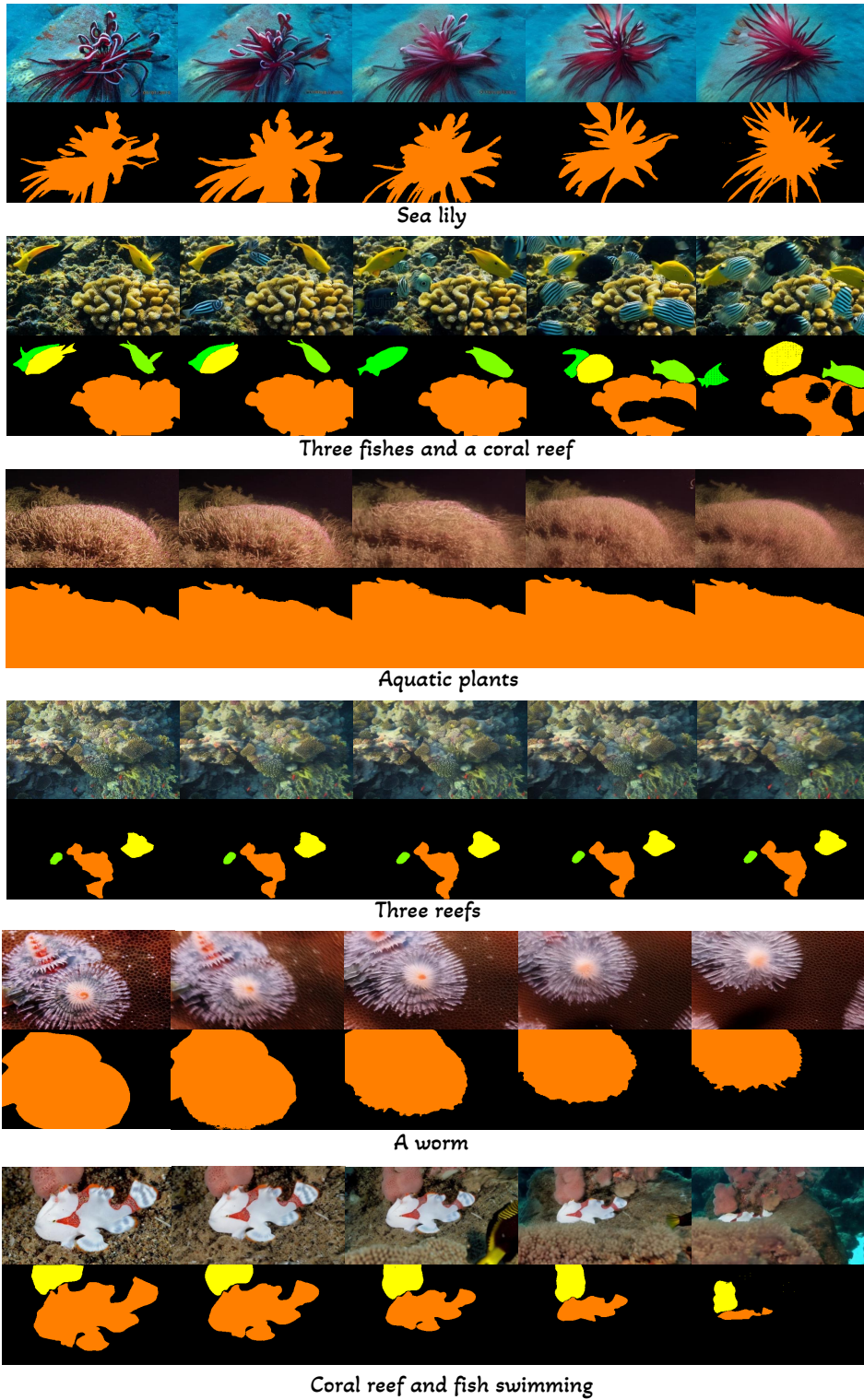


Figure 15. Additional samples generated from UTV with categories (from UIIS [10]) as text prompts.